Bridge-bonded adsorbates on fcc(100) and fcc(111) surfaces: A kinetic Monte Carlo study

C. G. M. Hermse,[1,*] A. P. van Bavel,[1] M. T. M. Koper,[2] J. J. Lukkien,[1] R. A. van Santen,[1] and A. P. J. Jansen[1,†]
[1]*Schuit Institute of Catalysis, ST/SKA, Eindhoven University of Technology, P.O. Box 513, 5600 MB Eindhoven, The Netherlands*
[2]*Leiden Institute of Chemistry, Leiden University, P.O. Box 9500, 2300 RA Leiden, The Netherlands*
(Received 4 January 2006; published 25 May 2006)

The adsorption of a bridge-bonded molecule onto fcc(100) and fcc(111) surfaces is studied using kinetic Monte Carlo simulations. The results are related to examples from both the electrochemical and the ultrahigh vacuum field. The lateral interaction model for the fcc(100) surface with the least excluded neighbor sites does not cause ordering in the adlayer at saturation coverage. This is due to the availability of two equivalent bridge sites per surface atom. The model with the most excluded sites on the other hand causes the formation of a $c(4\times2)$ ordered structure with a coverage of 0.25 ML. Surprisingly, for the model with intermediate-ranged lateral interactions a one-dimensionally ordered structure is found. In this one-dimensionally ordered structure, bridge-bonded anions are aligned along the $\sqrt{2}$ direction. The spacing between these rows varies, since each new row can form at either one of the two kinds of bridge site per surface atom. The local distribution between these one-dimensional rows can be described by, respectively, a $c(2\sqrt{2}\times\sqrt{2})$ or a $(\sqrt{2}\times\sqrt{2})$ unit cell [the latter one is also referred to as $c(2\times2)$]. On the fcc(111) surface, once again no ordered structure is found for the model with the smallest number of excluded sites. For the models with more excluded sites a $c(4\times2)$ ordered structure [also known as $c(2\times\sqrt{3})$] and a $(\sqrt{3}\times\sqrt{7})$ ordered structure are formed, the coverages being 0.50 and 0.20 ML, respectively. The simulated voltammograms generally show a broad peak due to adsorption in a disordered phase, and, if a two-dimensionally ordered structure is formed, a second sharp peak due to a disorder-order transition in the adlayer. The formation of the one-dimensionally ordered structure does not cause an additional current peak in the voltammogram.

DOI: 10.1103/PhysRevB.73.195422 PACS number(s): 68.43.Hn, 82.65.+r, 02.70.Uu

I. INTRODUCTION

The adsorption of anions on single-crystal electrode surfaces usually gives rise to the appearance of ordered adsorbate adlayers. The formation of these ordered adlayers is often accompanied by a characteristic sharply peaked current response in the cyclic voltammetry, commonly referred to as "butterfly" in the electrochemical community.[1,2] These adsorbed anions are, apart from their characteristic voltammetric response, also known to influence profoundly the electrochemical and structural properties of electrode surfaces. Adsorbed anions influence the reactivity, they may cause reorientation of the steps at the surface and suppress oxidation of the surface. They may cause, but also lift reconstructions of the surface. Finally, they can greatly enhance metal dissolution, or be involved in underpotential deposition (UPD).[3–5] Understanding these processes requires a thorough insight in the interactions between the anion and the surface and among the anions themselves, thus meriting theoretical study. Previous studies trying to model specific anion adsorption have treated atop and fourfold hollow adsorption of ions on fcc(100), atop and threefold hollow adsorption on fcc(111) surfaces, and more recently also bridge adsorption on fcc(111) surfaces.[6–10] From these studies it has become clear that the combination of the adsorption site and the lateral interactions defines the voltammogram shape and the ordered structure formed.

In extension to these studies, we give a more extensive treatment of bridge-bonded adsorption on fcc(100) and fcc(111) surfaces in the presence of lateral interactions. The distinguishing factors of the models considered here from top-, threefold-, and fourfold-bound adsorbates studied previously are that (1) the interaction model does not have the same symmetry as the underlying substrate and (2) there is more than one bridge site available per substrate atom. This second factor allows the system to choose between two energetically equivalent sites, and therefore introduces an extra degree of freedom. This may give rise to the formation of several different ordered or semiordered structures with all adsorbates on bridge sites, which are nevertheless energetically equivalent.

A detailed comparison of our model with experimental results yields the following observation. Seemingly very different molecules, from halides to small inorganic molecules (NO, CO), and even small organic molecules (urea), behave in a similar fashion. This similar behavior is observed for two very different adsorption processes; gas phase adsorption (under UHV, of CO, NO, and halides) and in aqueous solution (electrosorption of urea, sulfate, and halides). It even holds for two different surface topologies, a hexagonal and a square one. The current study ties these seemingly very different molecules and conditions together for the first time. The very general implication is that the overall adsorption kinetics and the ordering behavior of all these molecules is determined by the type of site it adsorbs on in combination with the lateral interaction model. The specific nature of the molecule or the phase from which it adsorbs is less important. This conclusion has a broad focus, and can contribute to other systems where spontaneous ordering or self-organization occurs.

II. MODEL

We model the electrosorption of an anion A from a solution onto a surface by Monte Carlo simulations employing a lattice-gas model for the substrate

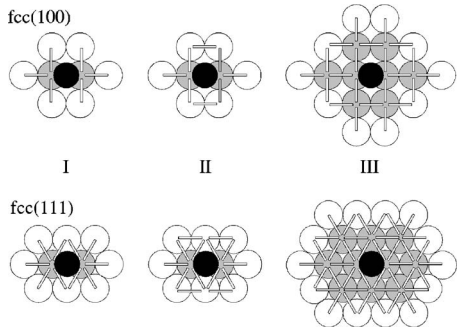

FIG. 1. Lateral interaction models treated in this work. Top left, model I: the adsorbed anion (black circle) binds to a bridge site on the fcc(100) surface, making bonding to the first shell of neighboring atoms (gray circles) impossible. The blocked bridge sites are indicated by the white rectangles. Top center, model II, is similar to model I, with additional exclusion of the bridge sites located at one lattice distance. Top right, model III: the adsorbed anion binds to a bridge site on the surface, making bonding to the first and second shell of neighboring atoms impossible. Bottom left: the adsorbed anion binds to a bridge site on the fcc(111) surface, making bonding to the first shell of neighboring atoms impossible. Bottom center: additional exclusion of the bridge sites located at one lattice distance. Bottom right: the adsorbed anion binds to a bridge site on the surface, making bonding to the first and second shell of neighboring atoms impossible.

$$A^{1-} + * * \leftrightarrows A_{\mathrm{ads}} + e^{-}, \tag{1}$$

where ** denotes an empty bridge site (formed by two empty surface atoms); each * corresponds to a surface atom.

Alternatively, we are interested in the adsorption of a molecule A from the gas phase

$$A_{\mathrm{gas}} + * * \leftrightarrows A_{\mathrm{ads}}. \tag{2}$$

Figure 1, top part, shows the (100) substrate and the neighboring sites around a central bridge-bonded adsorbate (in black). We consider a shell of purely hard interactions, in which the simultaneous bonding of two anions to neighboring sites is simply excluded. These excluded neighboring sites are displayed in white in Fig. 1. The exclusion of the first (and sometimes also second) shell of neighboring sites is a common approximation related to the fact that the metal-metal distance is usually smaller than the Van der Waals diameter of the adsorbate.[7,10,11] Significant repulsion is therefore expected if two adsorbates bind this close together. A similar exclusion of neighboring bridge sites is modeled for the anion on a fcc(111) surface, see the bottom part of Fig. 1.

The isotherms were calculated by determining the coverage θ on the lattice as a function of the electrode potential E. For this purpose, we carried out kinetic Monte Carlo simulations using the program CARLOS.[12,13] The isotherms were calculated by including adsorption, desorption and surface diffusion steps, and scanning E.

Sweeping the potential E corresponds to shifting the adsorption-desorption equilibrium during electrosorption. An electrochemical adsorption experiment by shifting the electrode potential can be related to adsorption from the gas phase by changing the reactant pressure. In the former case one has for the ratio of the adsorption to the desorption rate constant $k_{\mathrm{ads}}/k_{\mathrm{des}}$

$$k_{\mathrm{ads}}/k_{\mathrm{des}} = C' \exp\left(-\frac{\gamma e E}{k_{\mathrm{B}}T}\right), \tag{3}$$

which is proportional to the electrode potential E (γ is the electrosorption valency), whereas in the latter case one has

$$k_{\mathrm{ads}}/k_{\mathrm{des}} = C'' P_{\mathrm{A}}, \tag{4}$$

with P_A the gas phase pressure of molecule A.

The algorithm used was the first reaction method. In this algorithm, a tentative time is calculated for every possible reaction. All reactions together with their tentative times are stored in an event list. The algorithm proceeds by repeatedly performing the following steps: select the reaction with minimal time from the event list, advance the system time to the time of this reaction, adjust the lattice according to the reaction, and update the event list. For the case of time-dependent rate constants (such as in voltammetry, where rate constants are time dependent because of the time dependent potential), one can determine the tentative times exactly or approximate them by taking the rate constants constant for a small time step. In this work the times were determined exactly. We have used kinetic Monte Carlo simulations rather than equilibrium Monte Carlo simulations to allow us to study also the nonequilibrium adsorption of anions, which is important for high sweep rates. The rate constants for adsorption and desorption are

$$k_{\mathrm{ads}} = k^0 \exp\left(\frac{-\alpha_{\mathrm{ads}}\gamma e E}{k_{\mathrm{B}}T}\right), \tag{5}$$

$$k_{\mathrm{des}} = k^0 \exp\left(\frac{\alpha_{\mathrm{des}}\gamma e E}{k_{\mathrm{B}}T}\right), \tag{6}$$

where $\alpha_{\mathrm{ads}} = 1/2$ is the transfer coefficient for adsorption, γ is the electrosorption valency (taken as -1), e is the elementary charge, and E is the electrode potential. The exponent describes the potential-dependent adsorption of the anion. The definitions in Eqs. (5) and (6) imply that in our model at zero potential the adsorption rate constant is equal to the desorption rate constant: $k_{\mathrm{ads}} = k_{\mathrm{des}} = k^0$. The transfer coefficient for desorption is given by

$$\alpha_{\mathrm{des}} = 1 - \alpha_{\mathrm{ads}}. \tag{7}$$

The potential-independent diffusion steps were defined as hopping between neighboring bridge sites.

Apart from the coverage-voltage (θ-E) isotherm itself, we are particularly interested in the compressibility $d\theta/dE$ of the adlayer, as this quantity is proportional to the Faradaic current measured in an electrochemical voltammetry experiment

$$j = -e\gamma\Gamma_m \nu \frac{d\theta}{dE}, \tag{8}$$

where j is the Faradaic current in $\mathrm{A/cm^2}$, Γ_m is the number of surface sites per unit surface area [taken to be 1.5

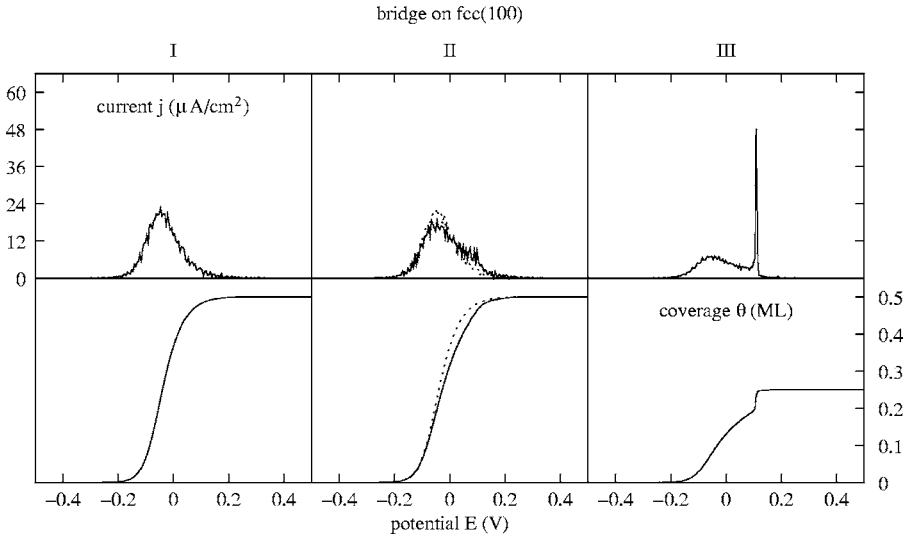

FIG. 2. Comparison of the simulated voltammogram (top) and adsorption isotherm (bottom) for the models of a bridge-bound anion on a fcc(100) lattice. The dotted line in the center panel for model I is added for easy comparison with the solid line in the center panel for model II.

$\times 10^{15}$ sites/cm^2 for both the (111) and (100) surface], and ν is the sweep rate (typically 25 mV/s). The adsorption current is proportional to the adsorption rate since

$$\frac{d\theta}{dE} = \frac{d\theta}{dt}\frac{1}{\nu}. \tag{9}$$

The voltammograms (current/potential plots) in the following sections may therefore also be interpreted as adsorption rates during an adsorption experiment where the surface coverage is in equilibrium with the gas phase, and the reactant pressure is slowly increased. Each potential shift of 0.1 V at room temperature corresponds to an approximate increase in the gas phase pressure of molecule A with a factor 50.

The voltammograms shown here are averages over four individual simulations on a 256×256 lattice with periodic boundary conditions, to increase the signal-to-noise ratio. The temperature was fixed at 300 K. The compressibility $d\theta/dE$ of the adlayer was determined by taking the difference of the adsorption and the desorption rate for each time interval of 0.2 s and dividing it by the sweep rate. The disorder-order transition at 0.11 V in Fig. 2 is particularly sensitive to the level of equilibration; an insensitivity of this peak to reducing the sweep rate indicates that the surface is well equilibrated. The isotherms were therefore calculated by choosing the rates of adsorption, desorption, and diffusion such that upon reducing the sweep rate from 25 to 5 mV/s the disorder-order transition peak is shifted by less than 5 mV. The values fulfilling this requirement are $k^0=10^3$ s^{-1} and $k^0_{\mathrm{diff}}=10^5$ s^{-1}. Please note that the diffusion rate constant was modeled to be independent of the applied potential. Therefore there is no use in specifying both a prefactor and a diffusion barrier: we can suffice by defining only the effective value for the diffusion rate constant. The sweep rate used was 25 mV/s unless stated otherwise. The lattice of 256×256 sites is sufficiently large to minimize the occurrence of finite-size effects. This was tested by comparing the results of our simulations with both larger and smaller lattices. A change in lattice size does not influence the position of the disorder-order transition. All snapshots are 15×15 sites, taken from the full simulated grid of 256×256 sites. Due to the large size of the ordered domains, usually only one domain orientation is shown in the figures, but we wish to emphasize that all possible domain orientations are found when looking on the scale of the full simulated grid.

III. RESULTS

A. Bridge-bonded anions on fcc(100) surfaces

The adsorption isotherm and simulated voltammogram for model I of the bridge-bonded anion on a fcc(100) surface is displayed in the left panel of Fig. 2. Adsorption takes place between −0.2 and +0.2 V, causing one broad peak in the current. Due to the availability of two bridge sites per surface atom and the mild constrictions due to lateral interactions, the adsorbate configuration is not ordered at saturation (Fig. 3, left). The adsorption energy and saturation coverage of the disordered structure shown on the left and the one-dimensionally ordered structure shown in the middle of Fig. 3 are identical. However, the configurational entropy of the disordered structure is larger, and a disordered structure is therefore always found for model I.[11]

A small extension of the range of the lateral interactions yields model II. The adsorption for this model is slightly delayed with respect to model I, due to the larger range of the lateral interactions [compare the solid (model II) and the dotted (model I) line in the center panel]. Also, the adsorbates form a one-dimensionally ordered structure at saturation, as discussed below.

A typical adsorbate configuration for model II after saturation is shown in the middle part of Fig. 3. The adsorbates line up in rows, which extend along the direction indicated by the arrows. At first glance this may appear a clean two-dimensionally ordered adsorbate configuration. Closer inspection reveals that three different unit cells can be obtained: $c(2\sqrt{2}\times\sqrt{2})$, and two alternative $(\sqrt{2}\times\sqrt{2})$ structures. The ordered structure with the primitive $(\sqrt{2}\times\sqrt{2})$ unit cell (which is rotated with respect to the underlying lattice) is more commonly referred to as $c(2\times2)$, where the orientation of the unit cell coincides with the orientation of the underlying fcc(100) surface lattice. Patches of these three structures

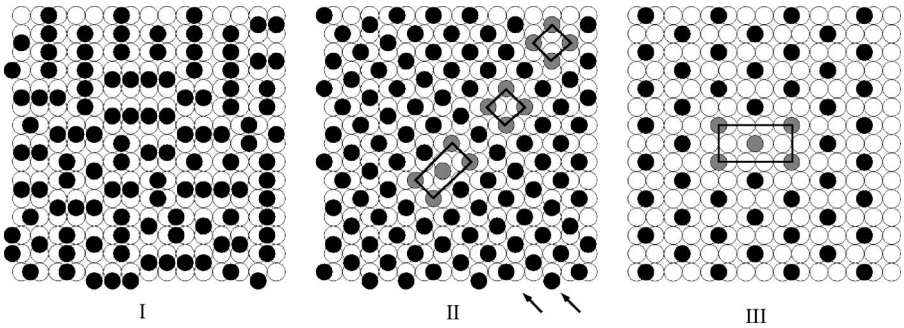

FIG. 3. Typical adsorbate configurations after adsorption for the models of a bridge-bound anion on a fcc(100) surface. For model I, no ordering is found. For model II, one-dimensional ordering along the direction of the arrows is found. Local patches will order into, respectively, a $c(2\sqrt{2}\times\sqrt{2})$, a $(\sqrt{2}\times\sqrt{2})$, and a $(\sqrt{2}\times\sqrt{2})'$ ordered structure (unit cells are indicated). The unit cell for the $c(4\times2)$ ordered structure found for model III is also indicated.

coexist on the surface. The patches are rectangular in shape, with the long sides in the direction of the arrow ranging over several hundred unit cells. The coexistence of these three ordered structures originates from the different way in which each type of bridge site (indicated *A* and *B* in Fig. 4) is occupied. For the $c(2\sqrt{2}\times\sqrt{2})$ ordered structure, these are alternatingly occupied *ABAB*…. For the two $(\sqrt{2}\times\sqrt{2})$ structures, only one type of bridge site is occupied, yielding either *AAA*… or *BBB*…. As can be seen from Figs. 4 and 5, pieces of all three ordered structures can readily be combined to fill the surface. Since the coverage and energy of all these structures is identical, their abundance is entropy driven: the chance that the next row consists of adsorbates bound to *A*-type bridge sites is equal to the chance that the next row consists of adsorbates bound to *B*-type bridge sites, 50%. Note that no separate disorder-order transition current peak is seen in the voltammogram for the formation of this one-dimensionally ordered structure.

In view of the experimental relevance of the $c(2\sqrt{2}\times\sqrt{2})$ and $(\sqrt{2}\times\sqrt{2})$ structure we have investigated what the effect is of additional finite interactions on their formation. It turns out that one additional interaction, indicated in gray in Fig. 7, controls the relative abundance of the $c(2\sqrt{2}\times\sqrt{2})$ and the $(\sqrt{2}\times\sqrt{2})$ structure (as shown in Fig. 6). If this interaction is more negative than −0.1 kT (−0.25 kJ/mol at room temperature), then only the $(\sqrt{2}\times\sqrt{2})$ structure is present. If this interaction is between +0.1 kT and +2 kT (0.25 and 5 kJ/mol at room temperature), then only the $c(2\sqrt{2}\times\sqrt{2})$ structure is present. For intermediate values of the interaction, both structures are found. For values of the lateral interaction larger than +2 kT, an additional ordered structure is found at 0.40 ML. This structure is described as $c(\sqrt{5}\times\sqrt{5})$. In the absence of finite lateral interactions the voltammogram shows only one broad adsorption peak. However, in the presence of repulsive lateral interactions larger than +0.25 kT (0.6 kJ/mol at room temperature) a clear disorder-order transition is visible in the voltammogram as a "spike," and a jump in coverage is seen in the adsorption isotherm.

Further increasing the range of lateral interactions causes a drop in the saturation coverage (model III, right part of Fig. 2), from 0.50 to 0.25 ML. The voltammogram now shows two peaks, one due to adsorption in a disordered phase, and

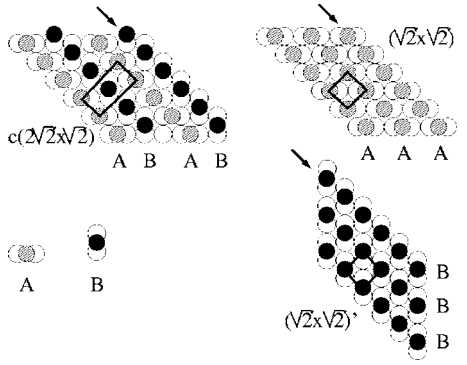

FIG. 4. The stacking of adsorbates [for model II on the fcc(100) surface] in the first direction is similar for the $c(2\sqrt{2}\times\sqrt{2})$, the $(\sqrt{2}\times\sqrt{2})$, and the $(\sqrt{2}\times\sqrt{2})'$ ordered structure: this direction is indicated by the arrows. The difference is in the second direction. In the $c(2\sqrt{2}\times\sqrt{2})$ ordered structure the two types of bridge sites are alternatingly occupied: *ABABAB*…. In the $(\sqrt{2}\times\sqrt{2})$ ordered structure only one type of bridge site is occupied: *AAA*…; in the alternative $(\sqrt{2}\times\sqrt{2})$ ordered structure, the other type of bridge site is occupied: *BBB*….

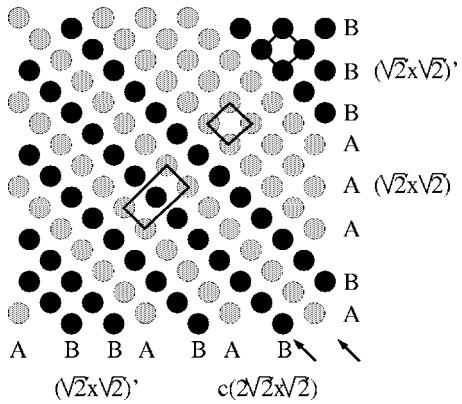

FIG. 5. The same adsorbate configuration as displayed in Fig. 3, middle panel, except now the substrate atoms have been left out, and the adsorbates are colored according to the type of bridge site they bind to. Gray circles denote type *A* adsorbates, black circles denote type *B* adsorbates. The unit cells of the various ordered structures are indicated, and the direction of the one-dimensional ordering is indicated by the arrows.

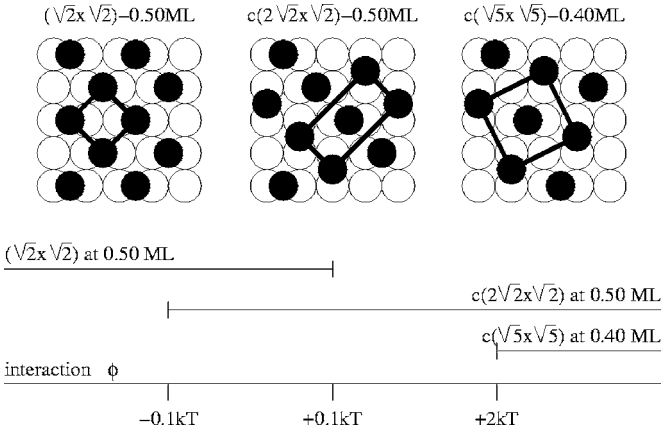

FIG. 6. Diagram showing which ordered structures are found as a function of the value of the lateral interaction φ defined in Fig. 7.

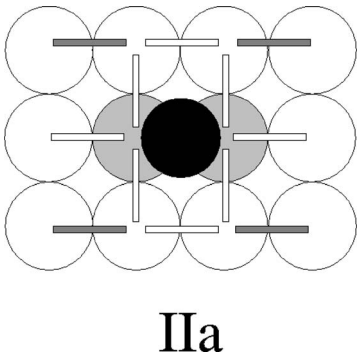

FIG. 7. Extended lateral interaction model, model IIa. The bridge sites indicated by the white rectangles are blocked by adsorption at the center bridge site. In addition, there is a finite repulsion or attraction φ with adsorbates bound to the bridge sites indicated in gray.

a second one at 0.11 V due to a disorder-order transition in the adlayer. This disorder-order transition transforms a disordered adlayer with a coverage of 0.20 ML into a $c(4\times2)$ ordered structure of 0.25 ML coverage (right part of Fig. 3).

B. Bridge-bonded anions on fcc(111) surfaces

The adsorption of bridge-bonded anions for model I on the fcc(111) surface (left part of Figs. 8 and 9) shows very similar behavior to the adsorption for model I on the fcc(100) lattice. Adsorption takes place between −0.2 and +0.2 V, causing one broad adsorption peak. The adlayer at saturation is disordered, due to the choice between the three different bridge sites per surface atom and the mild constrictions of the lateral interaction model. The adsorption energy and saturation coverage of the disordered structure shown on the left and the ordered structure shown in the middle of Fig. 9 are identical. However, the configurational entropy of the disordered structure is larger, and a disordered structure is therefore always found for model I.[11]

A small extension of the range of excluded sites, as defined on model II, again causes ordering of the adlayer. This time the ordering is two dimensional, while for the fcc(100) surface the ordering is one dimensional. The ordered structure formed is a $c(4\times2)$ structure, which is also referred to as $c(2\times\sqrt{3})$ (middle of Fig. 9). This structure is formed during a disorder-order transition at 0.18 V, and is associated with an increase in coverage from 0.45 to 0.50 ML. The disorder-order transition is clearly visible in the voltammogram as an additional sharp peak in the current.

Finally, for model III, the saturation coverage is reduced to 0.20 ML because of the larger number of excluded sites around each adsorbate. The simulated voltammogram once again displays a broad peak due to adsorption in a disordered phase, and a second sharp one due to a disorder-order transition in the adlayer (right part of Figs. 8 and 9). The disorder-order transition (at 0.22 V) converts the disordered adlayer with a coverage of 0.18 ML into the saturation ordered $(\sqrt{3}\times\sqrt{7})$ structure with a coverage of 0.20 ML. This system has been described previously because of its similarity to sulfate adsorption on the fcc(111) surfaces on many metals.[10,14]

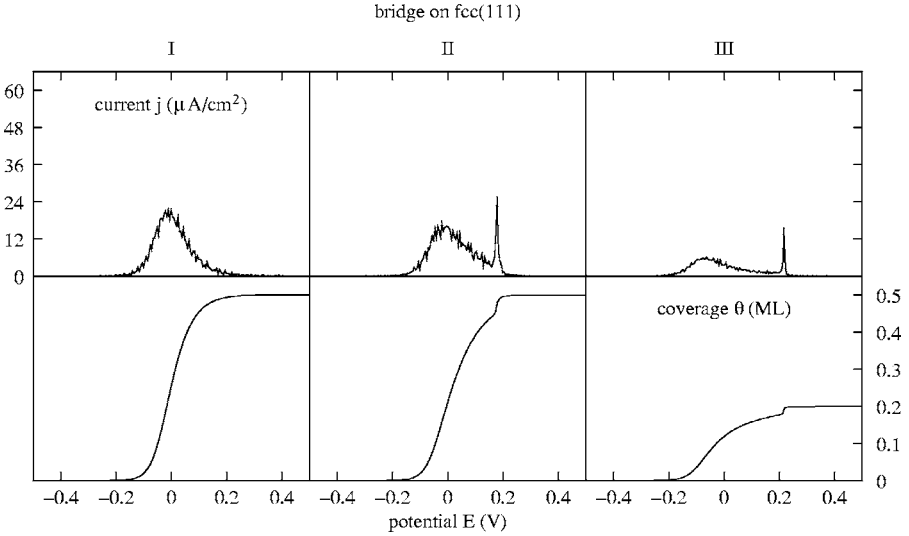

FIG. 8. Comparison of the simulated voltammogram (top) and adsorption isotherm (bottom) for the models of a bridge-bonded anion on a fcc(111) lattice.

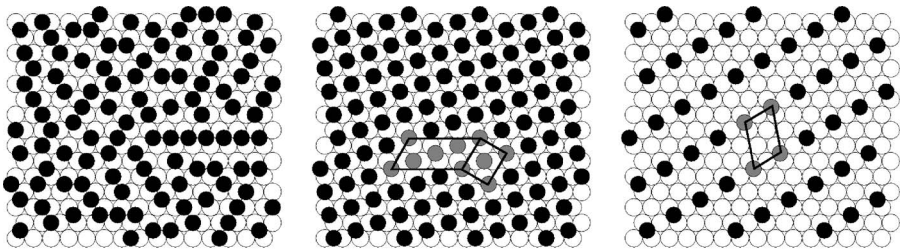

FIG. 9. Typical adsorbate configurations after adsorption for the models of a bridge-bonded anion on a fcc(111) surface. For model I, no ordering is found. For model II and III, a $c(4\times2)$ structure [also known as a $c(2\times\sqrt{3})$ structure] and a $(\sqrt{3}\times\sqrt{7})$ ordered structure are found, respectively. The unit cells are indicated for each structure.

IV. COMPARISON WITH EXPERIMENT

A. Adsorption on the fcc(100) surface

Several systems have been studied experimentally where the adsorbed molecule is bonded in a bridging fashion to the metal substrate. Below we will discuss some examples relevant to our simulation results.

Lateral interaction model II on the fcc(100) surface causes the formation of a $c(2\sqrt{2}\times\sqrt{2})$ and a $(\sqrt{2}\times\sqrt{2})$ structure at a coverage of 0.50 ML. Model I, which does not exclude the bridge sites located at one lattice distance from the adsorbate, has the same saturation coverage, but there is no ordering in the adsorbate layer. The results furthermore indicated that for small additional repulsions as indicated in Fig. 7 the $c(2\sqrt{2}\times\sqrt{2})$ structure dominates, while for small additional attractive interactions the $(\sqrt{2}\times\sqrt{2})$ structure is most abundant. In the absence of the finite additional interaction both ordered structures are found for model II.

The $c(2\sqrt{2}\times\sqrt{2})$ ordered structure is found for bromide (Br^-) electrosorption as well as for dissociative bromine gas (Br_2) adsorption on Au(100).[4,15–18] In the electrochemical case, the coverage can be further increased by increasing the electrode potential, and an additional incommensurate structure is formed. This incommensurate structure cannot be reproduced in our model, but has been recently simulated using off-lattice Monte Carlo.[19] The binding site was confirmed to be bridge by two independent DFT studies.[19,20] The voltammogram for bromide adsorption is dominated by the deconstruction of the reconstructed gold surface. It is therefore not possible to compare to our simulation results.

Chloride and iodide ions have also been investigated on Au(100).[15,21] The chloride ions, because they are much smaller, experience less repulsive interactions. The $c(2\sqrt{2}\times\sqrt{2})$ ordered structure is therefore not found, only an incommensurate structure with a coverage of over 0.50 ML. The iodide ions on the other hand are larger than the bromide ions. For this case it was reported that by stepping up the electrode potential coverages, close to 0.50 ML could be reached, and subsequently a $c(2\sqrt{2}\times\sqrt{2})$ ordered structure was found.

Halide adsorption on the Pt(100) surface yields, in contrast to the results on gold, a mixture of the $c(2\sqrt{2}\times\sqrt{2})$ and the $(\sqrt{2}\times\sqrt{2})$ structure. Studies for bromide adsorption on Pt(100) report "difficulty to find large two-dimensionally ordered domains,"[22] "locally ordered structures,"[23] and "partially ordered structures, consisting of quasihexagonal elements as well as rectangular ones."[24] In the last description, the quasihexagonal elements refer to parts of the $c(2\sqrt{2}\times\sqrt{2})$ structure, while the rectangular ones refer to the $(\sqrt{2}\times\sqrt{2})$ structure. In addition to electrosorbed bromide, people have also looked at the adsorption of hydrogen bromide (HBr). This molecule produces a $c(2\sqrt{2}\times\sqrt{2})$ structure.[25] Studies of iodide electrosorption indicate the formation of a $c(2\sqrt{2}\times\sqrt{2})$, a $(\sqrt{2}\times\sqrt{2})$ ordered structure or a combination of the two.[5,26,27]

From the comparison between the halide adsorption behavior on these two metal surfaces one might induce that the repulsion between the halide ions is weaker on gold than on platinum. The difference in the repulsion for these two metal surfaces may be related to the difference in lattice distance: 3.92 Å for Pt vs 4.08 Å for Au. Finally, it is interesting to note that a first-principles study of the coverage-dependent binding energy of chloride ions on bridge sites of the Ag(100) surface fully supports the choice of excluded sites in interaction model II (we accept that chloride normally resides in fourfold sites on this surface, but the calculations were also performed for the bridge sites).[28]

Carbon monoxide (CO) adsorbed on the (100) surface of palladium also forms a $c(2\sqrt{2}\times\sqrt{2})$ structure. The binding site has been confirmed to be bridge using DFT calculations, IR and EELS measurements.[29–33] For CO on platinum a $(\sqrt{2}\times\sqrt{2})$ ordered structure is formed. This case is less straight forward, since there is only a small difference in binding energy between the top and the bridge site. The LEED pattern may therefore be due to either $(\sqrt{2}\times\sqrt{2})$ islands of top bound CO molecules, or islands of bridge bound CO molecules, or a combination of the two.[30,34–36] A similar effect has been noticed for CO on Rh(100) and Ni(100), where also $(\sqrt{2}\times\sqrt{2})$ ordered structures are formed with either top- or bridge-bound adsorbates. In this case the difference in energy between top and bridge site is so small, that coadsorption with hydrogen induces a change in the type of site occupied by CO.[33,37]

Lateral interaction model III on the fcc(100) surface causes the formation of a $c(4\times2)$ ordered structure with a coverage of 0.25 ML. The voltammogram shows two peaks, one due to adsorption in a disordered phase, and a second one due to a disorder-order transition in the adlayer.

The electrosorption of urea on Pt(100) shows a sharp peak

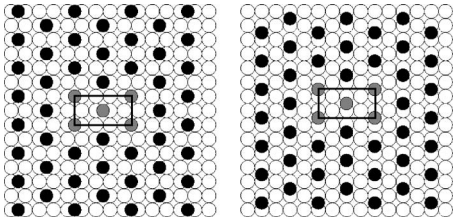

FIG. 10. Models for the $c(4\times2)$-0.25 ML ordered structure found for urea electrosorption on Pt(100). Left: model consistent with lateral interaction model III. Right: model proposed by Rikvold *et al.* The urea molecules in both models are located two lattice vectors away from each other. However, each urea molecule binds through two nitrogen atoms to the substrate atoms. Due to the different orientation of the urea molecules, the distance between nitrogen atoms of neighboring urea molecules is different for both models. For our model on the left this distance is always equal to or larger than $\sqrt{2}$ lattice vectors, while for the model by Rikvold *et al.* it is as small as one lattice vector.

in the voltammogram, and *ex situ* a $c(4\times2)$ ordered structure can be detected by means of LEED.[38,39] In the adsorption reaction two electrons are transferred per urea molecule, and the urea is bonded in a bridging fashion with both nitrogen atoms attached to the surface. The adsorption of urea coincides with the desorption of adsorbed hydrogen; the sharp voltammetric peak is thought to be due to the interactions between adsorbed urea and hydrogen during the conversion of the hydrogen atom adlayer into a urea adlayer.[40] The formation of this ordered structure has been studied previously by the group of Rikvold.[8,38,41] Their results could very well reproduce a $c(4\times2)$ ordered structure, as well as the sharp adsorption peak in the corresponding voltammogram. An interesting observation with regard to the model by these authors, is that in their $c(4\times2)$ ordered structure, the urea molecules are located two lattice vectors away from each other, but since each urea molecule binds through two nitrogen atoms, the distance between the nitrogen atoms of neighboring urea molecules is only one lattice vector. We suspect that significant repulsion between these nitrogen atoms will arise at such small separations. In our model of the $c(4\times2)$ structure, the distance between the nitrogen atoms of neighboring urea molecules is larger, $\sqrt{2}$ lattice vectors or more. This is because even though the distance between the individual urea molecules is the same, the orientation of the molecules is different for the two models. The difference between the two models is indicated in Fig. 10. The low saturation coverage of urea (0.25 ML) already indicates that strongly repulsive interactions are present in the adlayer. These repulsive interactions will favor keeping the individual adsorbates as far apart as possible. We therefore suggest that the model by Rikvold *et al.* can be slightly adjusted to the one described by us as Model III for fcc(100) surfaces. Please note that our results in Figs. 2 and 3 yield a plausible alternative for the ordered structure, but the number of electrons per adsorbate equals one instead of two, and that the lower, broad peak of the adsorption isotherm is not as sharp as in the experiment: the width is 100 mV for our model vs 10 mV for the experiment and the model by Rikvold *et al.* This is related to the fact that adsorption of hydrogen was not included in our model.

Next, we want to shift attention to the adsorption from the gas phase of NO on the Pt(100) surface. This system has been studied by many authors, and it has been clear from LEED measurements that a $c(4\times2)$ structure is formed on the unreconstructed surface.[42,43] Vibrational studies indicated that NO is bound at one type of site.[43–45] Recent electronic structure calculations clearly indicate that this must be the bridge type site.[46,47] Up to now there has been one direct observation of this $c(4\times2)$ structure, by STM, and this clearly indicated a coverage of 0.25 ML.[48] This coverage has more recently been confirmed by XPS.[49] There have been extensive discussions on the exact nature of the $c(4\times2)$ ordered structure, and other studies have suggested a different coverage of NO of 0.50 ML.[42,45,47,50] This coverage was proposed based on missing peaks in the LEED pattern, and the fact that on most other metals the saturation coverage of NO and CO is much higher than 0.25 ML. Notwithstanding these arguments we are of the opinion that the STM images presented in Ref. 48 are the most direct observation of the $c(4\times2)$ structure reported so far. Our model III for adsorption on fcc(100) surfaces thus also describes the case of NO adsorption on the Pt(100) surface.

B. Adsorption on the fcc(111) surface

Lateral interaction model II on the fcc(111) surface causes the formation of a $c(4\times2)$ ordered structure with a coverage of 0.50 ML. Model I, which does not exclude the bridge sites located at one lattice distance from the adsorbate, has the same saturation coverage, but there is no ordering in the adsorbate layer.

Several $c(4\times2)$ ordered structures have been reported in the literature. Some of these are formed by threefold-site bound adsorbates, others by bridge-bound adsorbates. In the case of CO on Pd(111), the bridge and threefold site are almost equal in energy.[51,52] Earlier studies proposed that the $c(4\times2)$ structure was formed by threefold-bound CO only.[52,53] However, more recent STM studies (partially by the same authors) indicate that in fact two types of $c(4\times2)$ islands coexist, one with bridge-bound CO, the other one with threefold-bound CO.[54] Other high-pressure vibrational spectroscopy studies also indicate that CO on Pd(111) may be bound both to the top and the bridge site.[55,56] As example of $c(4\times2)$ ordered structures formed by threefold-bound adsorbates only, one can mention the case of sulfur on Rh(111), and NO on Rh(111).[57,58] The formation of this ordered structure (with threefold bound adsorbates) was also previously modeled using kinetic Monte Carlo lattice gas models, for both the molecular adsorption from the gas phase and the electrochemical case of anion adsorption.[7,59] For bridge-bound adsorption this was previously modeled by Persson *et al.*[60]

Model III for bridge site adsorption on fcc(111) surfaces has recently been discussed because of its relevance to anion adsorption from sulfuric acid solutions.[2,6] It is only included here for comparison with the other models, and to complete the set of models with first and second neighbor exclusion. For an extensive discussion on the experimental relevance of this model the interested reader is referred to Ref. 10.

V. CONCLUSIONS

We have studied the adsorption onto bridge sites for the fcc(111) and fcc(100) surface. Depending on the lateral interaction model, one- or two-dimensionally ordered or even disordered adlayers exist at saturation. For the fcc(100) surface, a $c(4\times2)$ ordered structure is found with a saturation coverage of 0.25 ML. The adsorption isotherm for this case shows a jump in coverage due to a disorder-order transition in the adlayer. The disorder-order transition is also visible in the voltammogram, where it appears as a spike at a potential more positive than the one of the main adsorption peak.

If the lateral interactions do not extend as far, the saturation coverage increases up to 0.50 ML, and a one-dimensionally ordered structure is formed. This is composed of strips of a $c(2\sqrt{2}\times\sqrt{2})$ and strips of a $(\sqrt{2}\times\sqrt{2})$ structure [the latter structure is also referred to as $c(2\times2)$]. Attractive interactions between neighboring adsorbates at this coverage favor the formation of the $(\sqrt{2}\times\sqrt{2})$ structure, while repulsive interactions convert it into the $c(2\sqrt{2}\times\sqrt{2})$ structure. The adsorption isotherm is in this case a smooth curve, and the voltammogram shows only one broad peak.

For the fcc(111) surface, a $(\sqrt{3}\times\sqrt{7})$ ordered adlayer is formed at a coverage of 0.20 ML. With fewer excluded bridge sites, the saturation coverage rises to 0.50 ML, and a $c(4\times2)$ ordered structure is found. Both ordered structures are formed through a disorder-order transition in the adlayer. This transition is visible in the voltammogram as a sharp spike on the right side of the main adsorption peak. It also shows up in the adsorption isotherm as a jump in coverage.

The current research clearly shows the wide applicability of lattice gas models employing sensible lateral interaction modeling. The results of such models are meaningful for both surface electrochemical and ultrahigh vacuum adsorption studies, involving a large variety of adsorbed species that ranges from halides, sulfate, and urea to CO and NO. The use of these kinds of models and the realization that the combination of the binding site and the lateral interaction model determines the adsorption and ordering behavior can improve the understanding of adsorption processes in general.

*Corresponding author. Electronic mail: chretien@sg10.chem.tue.nl

†Electronic mail: tgtatj@chem.tue.nl

[1] J. Clavilier, in *Interfacial Electrochemistry, Theory, Experiment, and Applications*, edited by A. Wieckowski (Marcel Dekker, New York, 1999).

[2] A. M. Funtikov, U. Stimming, and R. Vogel, J. Electroanal. Chem. **428**, 147 (1997).

[3] O. M. Magnussen, Chem. Rev. (Washington, D.C.) **102**, 679 (2002).

[4] E. Bertel and F. P. Netzer, Surf. Sci. **97**, 409 (1980).

[5] C. M. Vitus, S.-C. Chang, B. C. Schardt, and M. J. Weaver, J. Phys. Chem. **95**, 7559 (1991).

[6] M. T. M. Koper, J. J. Lukkien, N. P. Lebedeva, J. M. Feliu, and R. A. van Santen, Surf. Sci. **478**, L339 (2001).

[7] M. T. M. Koper and J. J. Lukkien, Surf. Sci. **498**, 105 (2002).

[8] P. A. Rikvold, H. Gamboa-Aldeco, J. Zhang, M. Han, Q. Wang, H. L. Richards, and A. Wieckowksi, Surf. Sci. **335**, 389 (1995).

[9] L. Blum, D. A. Huckaby, and M. Legault, Electrochim. Acta **41**, 2207 (1996).

[10] C. G. M. Hermse, A. P. van Bavel, M. T. M. Koper, J. J. Lukkien, R. A. van Santen, and A. P. J. Jansen, Surf. Sci. **572**, 247 (2004).

[11] C. G. M. Hermse and A. P. J. Jansen, in *Catalysis*, Vol. 19, edited by J. J. Spivey (Royal Society of Chemistry, Cambridge, 2006).

[12] CARLOS is a general-purpose program, written in C, for simulating reactions on surfaces that can be represented by regular grids; an implementation of the First-Reaction Method and the Variable Stepsize Method, written by J. J. Lukkien.

[13] J. J. Lukkien, J. P. L. Segers, P. A. J. Hilbers, R. J. Gelten, and A. P. J. Jansen, Phys. Rev. E **58**, 2598 (1998).

[14] J. M. Orts, L. Blum, D. Huckaby, J. M. Feliu, and A. Aldaz, Abstr. Pap. - Am. Chem. Soc. **220**, 91 (2000).

[15] A. Cuesta and D. M. Kolb, Surf. Sci. **465**, 310 (2000).

[16] B. M. Ocko, O. M. Magnussen, J. X. Wang, and Th. Wandlowski, Phys. Rev. B **53**, R7654 (1996).

[17] B. M. Ocko, O. M. Magnussen, J. X. Wang, R. R. Adzic, and Th. Wandlowski, Physica B **221**, 238 (1996).

[18] Th. Wandlowski, J. X. Wang, O. M. Magnussen, and B. M. Ocko, J. Phys. Chem. **100**, 10277 (1996).

[19] S. J. Mitchell and M. T. M. Koper, Surf. Sci. **563**, 169 (2004).

[20] S. Wang and P. A. Rikvold, Phys. Rev. B **65**, 155406 (2002).

[21] X. Gao, G. J. Edens, F.-C. Liu, A. Hamelin, and M. J. Weaver, J. Phys. Chem. **98**, 8086 (1994).

[22] J. M. Orts, R. Gióme z, J. M. Feliu, A. Aldaz, and J. Clavillier, Langmuir **13**, 3016 (1997).

[23] N. M. Marković, C. A. Lucas, H. A. Gasteiger, and P. N. Ross, Surf. Sci. **365**, 229 (1996).

[24] A. M. Bittner, J. Wintterlin, B. Beran, and G. Ertl, Surf. Sci. **335**, 291 (1995).

[25] G. A. Garwood and A. T. Hubbard, Surf. Sci. **112**, 281 (1981).

[26] J. L. Stickney, S. D. Rosasco, B. C. Schardt, and A. T. Hubbard, J. Phys. Chem. **88**, 251 (1984).

[27] H. Baltruschat, U. Bringemeier, and R. Vogel, Faraday Discuss. **94**, 317 (1992).

[28] H. Fu, L. Jia, W. Wang, and K. Fan, Surf. Sci. **584**, 187 (2005).

[29] D. Loffreda, D. Simon, and P. Sautet, J. Chem. Phys. **108**, 6447 (1998).

[30] J. P. Biberian, Surf. Sci. **118**, 443 (1982).

[31] P. Uvdal, P.-A. Karlsson, C. Nyberg, S. Andersson, and N. V. Richardson, Surf. Sci. **202**, 167 (1988).

[32] J. N. Andersen, M. Qvarford, R. Nyholm, S. L. Sorensen, and C. Wigren, Phys. Rev. Lett. **67**, 2822 (1991).

[33] C. Nyberg, L. Westerlund, L. Jönsson, and S. Andersson, J. Electron Spectrosc. Relat. Phenom. **54/55**, 639 (1990).

[34] P. van Beurden, Ph.D. thesis, Eindhoven University of Technology, 2003.

[35] R. Martin, P. Gardner, and A. M. Bradshaw, Surf. Sci. **342**, 69 (1995).

[36] P. Gardner, R. Martin, M. Tüshaus, and A. M. Bradshaw, J. Electron Spectrosc. Relat. Phenom. **54/55**, 619 (1990).
[37] A. P. van Bavel, Ph.D. thesis, Eindhoven University of Technology, 2005.
[38] M. Gamboa-Aldeco, P. Mrozek, C. K. Rhee, A. Wieckowski, P. A. Rikvold, and Q. Wang, Surf. Sci. Lett. **297**, L135 (1993).
[39] C. K. Rhee, J. Electrochem. Soc. **139**, 13C (1992).
[40] V. Climent, J. M. Orts, J. M. Feliu, J. M. Pérez, and A. Aldaz, Langmuir **13**, 2380 (1997).
[41] P. A. Rikvold, J. Zhang, Y.-E. Sung, and A. Wieckowski, Electrochim. Acta **41**, 2175 (1996).
[42] H. P. Bonzel, G. Broden, and G. Pirug, J. Catal. **53**, 96 (1978).
[43] G. Pirug, H. P. Bonzel, H. Hopster, and H. Ibach, J. Chem. Phys. **71**, 593 (1979).
[44] W. F. Banholzer and R. I. Masel, Surf. Sci. **137**, 339 (1984).
[45] P. Gardner, M. Tüshaus, R. Martin, and A. M. Bradshaw, Surf. Sci. **240**, 112 (1990).
[46] Q. Ge and M. Neurock, J. Am. Ceram. Soc. **126**, 1551 (2004).
[47] A. Eichler and J. Hafner, J. Catal. **204**, 118 (2001).
[48] M.-B. Song, K. Momoi, and M. Ito, Jpn. J. Appl. Phys., Part 2 **36**, L1528 (1997).
[49] E. D. L. Rienks, J. W. Bakker, A. Baraldi, S. A. C. Carabineiro, S. Lizzit, C. J. Weststrate, and B. E. Nieuwenhuys, Surf. Sci. **516**, 109 (2002).
[50] Y. Y. Yeo, L. Vattuone, and D. King, J. Chem. Phys. **104**, 3810 (1996).
[51] P. Sautet, M. K Rose, J. C. Dunphy, S. Behler, and M. Salmeron, Surf. Sci. **453**, 25 (2000).
[52] D. Loffreda, D. Simon, and P. Sautet, Surf. Sci. **425**, 68 (1999).
[53] T. Gießel, O. Schaff, C. J. Hirschmugl, V. Fernandez, K.-M. Schindler, A. Theobald, S. Bao, R. Lindsay, W. Berndt, A. M. Bradshaw, C. Baddeley, A. F. Lee, R. M. Lambert, and D. P. Woodruff, Surf. Sci. **406**, 90 (1998).
[54] M. K. Rose, T. Mitsui, J. Dunphy, A. Borg, D. F. Ogletree, M. Salmeron, and P. Sautet, Surf. Sci. **512**, 48 (2002).
[55] S. Surnev, M. Sock, M. G. Ramsey, F. P. Netzer, M. Wiklund, M. Borg, and J. N. Andersen, Surf. Sci. **470**, 171 (2000).
[56] W. K. Kuhn, J. Szanyi, and D. W. Goodman, Surf. Sci. Lett. **274**, L611 (1992).
[57] J. Cerdá, A. Yoon, M. A. van Hove, P. Sautet, M. Salmeron, and G. A. Somorjai, Phys. Rev. B **56**, 15900 (1997).
[58] R. M. van Hardeveld, Ph.D. thesis, Eindhoven University of Technology, 1997.
[59] C. G. M. Hermse, F. Frechard, A. P. van Bavel, J. J. Lukkien, J. W. Niemantsverdriet, R. A. van Santen, and A. P. J. Jansen, J. Chem. Phys. **118**, 7081 (2003).
[60] B. N. J. Persson, J. Chem. Phys. **92**, 5034 (1990).